

## Three-dimensional endoscopic photoacoustic imaging based on multielement linear transducer array

Yi Yuan, Sihua Yang, and Da Xing<sup>a)</sup>

MOE Key Laboratory of Laser Life Science & Institute of Laser Life Science, College of Biophotonics, South China Normal University, Guangzhou 510631, People's Republic of China

(Received 26 March 2011; accepted 18 July 2011; published online 9 September 2011)

An implementation system of three-dimensional endoscopic photoacoustic imaging is presented. The developed endoscopic photoacoustic detector integrates a multielement linear transducer array, a reflective device, a Plexiglass tube, and ultrasonic coupling medium. To match with the acoustic impedance of Plexiglass tube, a glycerin solution with 45% volume percentage was used as the ultrasonic coupling medium. This ultrasonic coupling medium can decrease photoacoustic pressure transmission loss during the progress of photoacoustic signal propagation. The capability of the system for three-dimensional imaging was verified with chicken breast tissue. Furthermore, pig normal rectal tissue and mouse breast tumor tissue in an *ex vivo* cavity model were imaged by the system. The reconstructed three-dimensional photoacoustic image presented the structural information of normal and lesion tissue. The experimental results demonstrate the multielement-based endoscopic photoacoustic imaging system with inside-out laser exciting mode has the ability of reconstructing three-dimensional images of biology tissue. © 2011 American Institute of Physics. [doi:10.1063/1.3626789]

### I. INTRODUCTION

Endoscope technology has been applied to clinical examination of diseases, such as intestinal disease, arthropathy, and gastric disease. Nowadays, endoscope used in clinic includes ultrasound endoscope and optical coherence tomography-endoscope, etc. However, challenges still exist in these endoscope systems for extending applications. For example, ultrasound endoscope offers low contrast in pathologic region, so it is difficult to diagnose diseases at early stage. Optical coherence tomography-endoscope can fill the shortage of the ultrasound endoscope, but it has poor penetration depth owing to utilizing ballistic photons.<sup>1</sup> As a new noninvasive medical imaging modality, photoacoustic (PA) imaging technology combines the merits of both high optical contrast and high ultrasound resolution. It can achieve deep tissue images with fine resolution, and distinguish tissue components with different spectrum excitation.<sup>2-4</sup>

With excellent predominance of combining with optics and ultrasonics, PA effect can potentially be applied into the endoscope technology. Several groups have put efforts on the study of the endoscopic PA imaging and the corresponding endoscopic imaging systems have been developed. PA endoscopic probe was setup for 1D sensing by Viator *et al.*<sup>5</sup> PA endoscopy microscopy with a single ultrasonic transducer for PA signal detection was reported by Yang *et al.*<sup>6</sup> Intravascular PA imaging system using commercial intravascular ultrasound probe was developed by Sethuraman *et al.*, and it was used to reconstruct the three-dimensional PA image of coronary artery stents,<sup>7,8</sup> however, the three-dimensional PA scanning with commercial intravascular

ultrasound probe needs rotated and pulled back or pushed forward step by step.

Recently, we have developed a preclinical PA imaging endoscope based on acousto-optic coaxial system using ring transducer array.<sup>9</sup> Based on our previous study, an endoscopic PA imaging system using a multielement linear transducer array was designed and established to collect PA signals for three-dimensional endoscopic PA imaging. Compared to the ring transducer array, the multielement linear transducer array has higher resolution and better tomographic capacity in *z* axis direction. With a linear transducer array, the system needs to scan only one circle for three-dimensional PA imaging rather than be pulled back or pushed forward step by step. In our knowledge, it is the first time to use a multielement linear transducer array for three-dimensional endoscopic PA imaging with inside-out laser exciting mode. The endoscopic PA detector consists of a multielement linear transducer array, a reflective device, a Plexiglass tube and ultrasonic coupling medium. The chicken breast tissue was used to verify the three-dimensional imaging capability of the system. Furthermore, pig normal rectal tissue and mouse breast tumor tissue in an *ex vivo* cavity model were also imaged by the endoscopic PA imaging system.

### II. MATERIALS AND METHODS

The schematic of the experimental setup was shown in Fig. 1(a). An Nd:YAG laser (LS-2134, LOTIS TII, Belarus), operating at wavelength of 532 nm with 10 ns FWHM at repetition rate of 15 Hz, was used in the experiment as the light source. The laser was filtered by a variable slit to get a beam with rectangular cross section. With an optical cylindrical lens, the laser was focused into a line and the length of the line is 10 mm. The laser focusing line is reflected by a

<sup>a)</sup>Author to whom correspondence should be addressed. Fax: +86-20-8521-6052. Electronic mail: xingda@scnu.edu.cn.

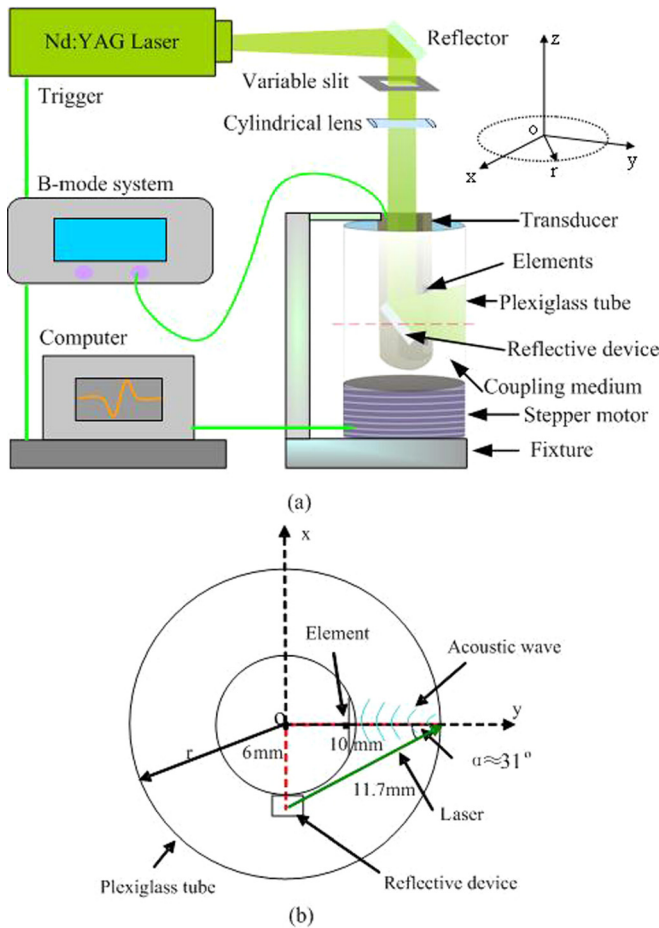


FIG. 1. (Color online) (a) The schematic of the experimental setup. (b) Profile of the endoscopic PA detector marked by the red dotted line shown in (a).

reflective device in the Plexiglass tube. Figure 1(b) is the profile of the endoscopic PA detector marked by the red dotted line shown in Fig. 1(a). In the experimental protocol, the reflective device was adjusted coarsely to make the reflected laser focusing line overlap with the ultrasonic focusing line in the tested sample. The multielement linear transducer array with a length of 50 mm and a width of 9 mm has 249 vertical sub-elements. The resonance frequency of the linear transducer array is 5 MHz. The transducer array is fixed by a fixture and remained stationary. The transducer array is enveloped by a Plexiglass tube which is 20 mm in diameter, and the Plexiglass tube is connected with a stepper motor. Test samples are put on the outer wall of the tube for PA imaging. Medical ultrasound gel is put between the outer wall and the tissue sample. It is conducive to the propagation of ultrasound from the tissue to the Plexiglass tube. To cover a  $2\pi$ -acceptance angle for the sample, the tube is driven by the stepper motor and a total of 100 steps with a constant  $3.6^\circ$  interval are taken. The experiment is conducted with an energy density of  $\sim 11 \text{ mJ/cm}^2$ .

The principle of the data collecting with the B-mode system has been reported by researches in the past.<sup>10,11</sup> A 15 Hz clock signal, provided by control circuit, was used for triggering the pulse laser and controlling sub-element of the linear transducer array to be dynamically selected to perform the linear scanning. A group of sub-elements gathered the

PA signals under the control of electric scanning switch off. Then multiway signals after preamplification were delivered to the dynamic focusing module for phase adjustment. Finally, the multiway signals were incorporated to one-way signal by delay and sum algorithm. When a group of sub-elements finished, the next group of sub-elements began to gather signals. The signals from the transducers are acquired with the data acquisition system (DAS) card (PCI-6541, NI, USA). The card features a high-speed 12-bit analog-to-digital converter with a sampling rate of 40 MHz. The system operation and data acquisition are controlled by a personal computer.

When transducer array captures PA signals without rotated scanning, one B-scan PA image along  $r$  direction of the tested sample can be obtained. When the transducer array captures PA signals from the entire circumference with scanning, PA tomography in  $x$ - $y$  plane can be reconstructed by different groups of sub-elements. Three-dimensional PA image is composed by a 3 D-Med software (Institute of Automation, Chinese Academy of Sciences) using the multiple PA tomography.

### III. RESULTS

#### A. Matching of the acoustic impedance

Normally, water was used as the ultrasonic coupling medium to propagate ultrasound for the PA imaging. However, the acoustic impedance of the Plexiglass tube is mismatch with the water in this system. The acoustic impedance of the Plexiglass tube and water are  $2.1 \times 10^6 \text{ Pa}\cdot\text{s/m}$  and  $1.5 \times 10^6 \text{ Pa}\cdot\text{s/m}$ , respectively. If acoustic impedance of the two medium is different, the intensity of the acoustic pressure will be attenuated. The pressure attenuation is called transmission loss (TL). TL is the decibel quantity of the acoustic pressure intensity ratio between the incident acoustic wave and the transmission acoustic wave. It obeys the following formula expressed by the acoustic impedance:

$$TL = -10 \log_{10} \left[ \frac{4Z_1 Z_2}{(Z_1 + Z_2)^2} \right], \quad (1)$$

where  $Z_1$  and  $Z_2$  are the acoustic impedance of one medium and the other medium, respectively. TL will weaken the intensity of PA signal received by the transducer. In order to satisfy matching condition of the acoustic impedance, the intensity of PA signal was measured under the same condition using ultrasonic coupling medium with different glycerol and water in volume percentage. The experimental result in Fig. 2 shows that TL is least when the glycerol is 45% in volume.

#### B. Estimating the spatial resolution of the system

Spatial resolution is an important parameter to imaging system. It is known that the resolution in  $r$  direction mainly depend upon the frequency response and bandwidth of the elements. In theory, the resolution in  $r$  direction can be estimated by the following formula:<sup>12</sup>

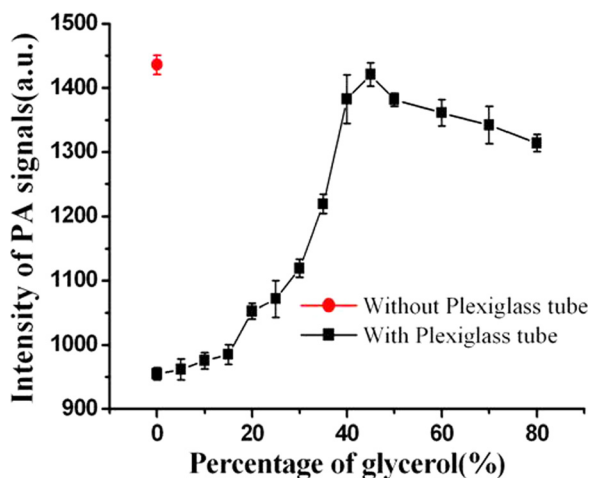


FIG. 2. (Color online) Curve diagram of the PA intensity vs different concentration of glycerin solution. The transmission loss was least when the volume percentage of the glycerol was 45%.

$$\Delta r \geq 1.5 \frac{c}{f_{\max}}, \quad (2)$$

where  $\Delta r$  is the resolution in  $r$  direction,  $c$  is the sound speed, and  $f_{\max}$  is the maximum frequency. The transducer array has a 5 MHz central frequency and a 70% nominal bandwidth. The  $f_{\max}$  of the transducer array is 6.75 MHz, and the  $c$  is  $\sim 1500$  m/s, therefore, we can obtain  $\Delta r \geq 0.36$  mm. In order to estimate the resolution in  $z$  axis direction, two carbon bars

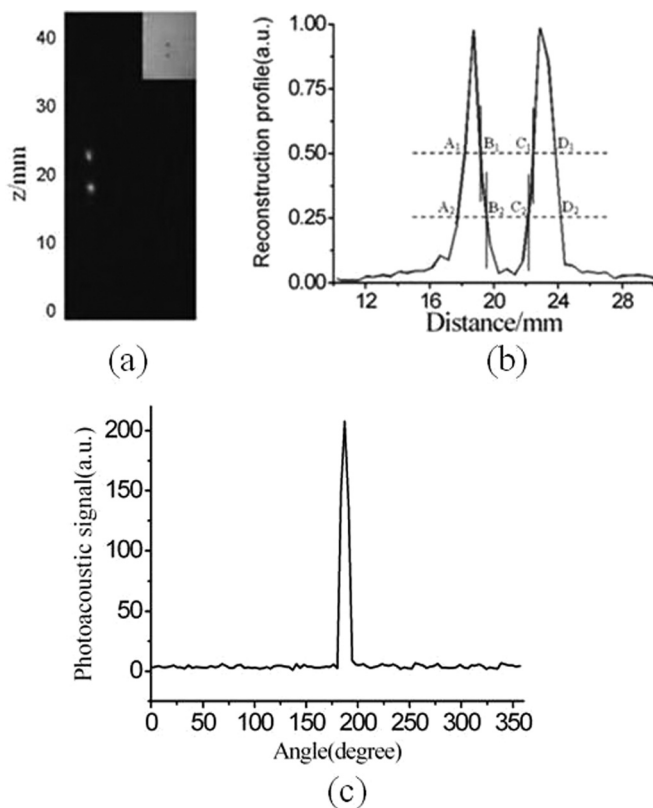


FIG. 3. (a) Reconstructed image of two carbon bars inserted in the transparent gelatin. (b) The normalized line profile of the reconstructed image shown in (a). The half-amplitude line and quarter-amplitude line cut across the profile at points  $A_1, B_1, C_1, D_1$  and  $A_2, B_2, C_2, D_2$ , respectively. (c) Lateral PSF of the hair.

with the diameter of 0.7 mm inserted in the transparent gelatin were used. Figure 3(a) shows the reconstructed image of the two carbon bars. Figure 3(b) shows the normalized line profile of the reconstructed image. The half-amplitude line and quarter-amplitude line cut across the profile at points  $A_1, B_1, C_1, D_1$  and  $A_2, B_2, C_2, D_2$  in Fig. 3(b). The resolution in  $z$  axis direction is equal to the summation of the distance between point  $B_1$  and  $B_2$  and the distance between point  $C_1$  and  $C_2$ .<sup>13</sup> The resolution in  $z$  axis direction was estimated to be  $\sim 0.4$  mm. In order to estimate resolution in  $x$ - $y$  plane, a hair with the diameter of  $53 \mu\text{m}$  was used in the experiment, the hair was fixed on the outer wall of the Plexiglass tube and rotated by the stepper motor, and then the PA signals generated from the hair were collected by the transducer. Figure 3(c) shows the lateral point spread function (PSF) of the hair. The FWHM (-6dB) lateral resolution in  $x$ - $y$  plane was determined by the lateral PSF.<sup>1</sup> The resolution in  $x$ - $y$  plane is  $\sim 1.9$  mm.

### C. Three-dimensional endoscopic PA imaging for biological tissue *ex vivo*

In order to demonstrate the three-dimensional imaging effect of the endoscopic PA imaging system, a trapezoid *ex vivo* chicken breast tissue with uniform thickness was tested in the experiment. Figure 4(a) is the photography of the *ex vivo* chicken breast tissue. The PA signals generated by the tissue were received by the elements. B-scan PA image was reconstructed by limited-field filtered-back projection algorithm.<sup>14</sup> Figure 4(b) is the B-scan PA images along  $r$ -direction of the chicken breast tissue marked by the red dotted line shown in Fig. 4(a). We calculate that the thickness of the chicken breast tissue is about 1 mm, which is consistent with the actual thickness. Figure 4(c) is three-dimensional PA

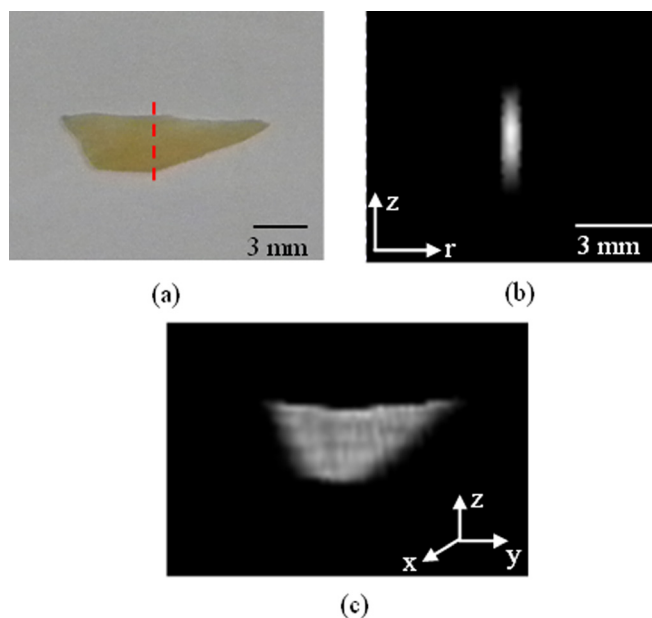


FIG. 4. (Color online) (a) Photography of the *ex vivo* chicken breast tissue. (b) Reconstructed B-scan PA images along  $r$  direction of the chicken breast tissue marked by the red dotted line shown in (a). (c) Reconstructed three-dimensional PA image of the chicken breast tissue (enhanced online) [URL: <http://dx.doi.org/10.1063/1.3626789.1>].

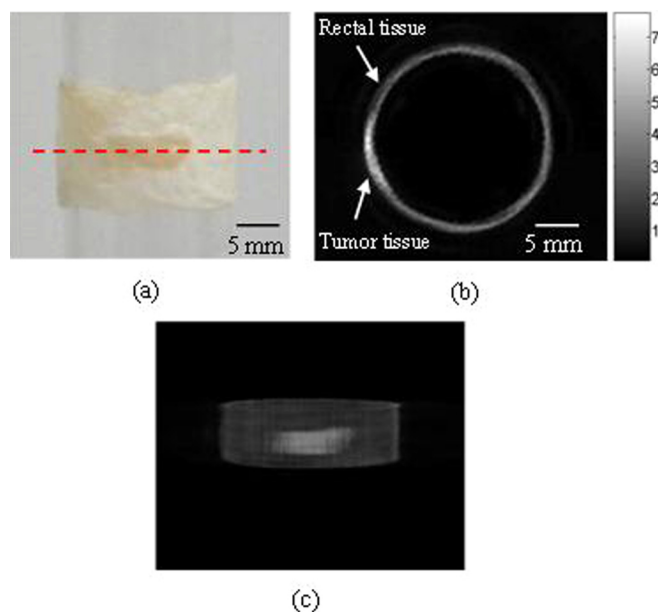


FIG. 5. (Color online) (a) Photography of the *ex vivo* cavity model made by pig normal rectal tissue and mouse breast tumor tissue. (b) Reconstructed PA tomography of the cavity model marked by the red dotted line shown in (a). (c) Three-dimensional PA image of the pig normal rectal tissue and the mouse breast tumor tissue (enhanced online) [URL: <http://dx.doi.org/10.1063/1.3626789.2>].

reconstructed image of the chicken breast tissue, which is in good agreement with the sample. Video 1 shows the reconstructed three-dimensional PA image rotating around the  $z$  axis, helping us to better understand the spatial orientation of the sample (see Fig. 4 caption for the link to (Video 1)). The experiment result indicates that the imaging system has the ability of fast reconstructing the three-dimensional structure of tissues with high contrast.

An *ex vivo* cavity model, which was made of pig normal rectal tissue and mouse breast tumor tissue, was used to verify that the system can be used to image both normal tissue and lesion tissue. The pig normal rectal tissues were obtained from the health pig and the mouse breast tumor tissue was excised from a nude mouse with the murine mammary tumor. The removed tissues were immediately and briefly rinsed in saline to remove excess blood on surface. The photography of the tissues fixed on the outer wall of Plexiglass tube is shown in Fig. 5(a). Figure 5(b) is the reconstructed PA tomography of the *ex vivo* cavity model using circular scanning, and the corresponding section was marked by the red dotted line shown in Fig. 5(a). Clearly, the contrast of the mouse breast tumor tissue is higher than that of the pig normal rectal tissue. The contrast ratio of mouse breast tumor tissue and pig normal rectal tissue is  $\sim 2.3$ . It is calculated by the ratio of pixel values shown in the shaded bar. The three-dimensional PA image of the pig normal rectal tissue and mouse breast tumor tissue is shown in Fig. 5(c). A satisfactory match between the photograph and the reconstructed image can be seen. Nonuniform contrast is shown in the three-dimensional PA image of the tumor tissue in Fig. 5(c), and it is probably caused by the optical absorption difference existing in the non-homogenous tumor tissue. We also recorded a video showing the three-dimensional struc-

tural information of the rectal tissue and tumor tissue (see Fig. 5 caption for the link to (Video 2)). The results demonstrate that the system can reconstruct the image of normal and lesion tissue.

#### IV. DISCUSSION

All of the experimental results show that the three-dimensional PA images can be reconstructed with high contrast by the endoscopic PA imaging system. However, the length limitation of laser focusing line reduces the imaging range. In order to obtain a wider imaging range, the length of laser focusing line would be expanded by reasonable optical beam shaping method. Obviously, the current structure and configuration of the PA detector still can not be used for real *in vivo* endoscopic imaging. For *in vivo* three-dimensional endoscopic photoacoustic imaging, the current system should be improved. Firstly, the light can be directed into a fiber optic bundle, which provided lateral light emission. The fiber optic bundle is distributed on a circumference with the same interval. The light from the fiber optic bundle is formed into a uniform cylinder beam to irradiate the tested sample. Secondly, the size of multielement linear transducer array should be reduced so that the transducer can be applied in imaging the *in vivo* sample. Thirdly, the linear transducer array will be rotated by a motor to capture the PA signals of the *in vivo* sample. Human rectal tumor tissue has stronger optical absorption than human normal rectal tissue at the wavelength of 532 nm.<sup>15,16</sup> Based on the different optical absorption between human normal rectal tissue and rectal tumor tissues, the *in vivo* three-dimensional endoscopic PA imaging system may be applied in reconstructing the three-dimensional PA images of normal and lesion tissue with high contrast.

#### V. CONCLUSIONS

In summary, an endoscopic PA imaging system has been developed with several attractive capabilities. Firstly, the inside-out laser exciting mode makes the PA imaging system feasible to realize the endoscopic imaging. Secondly, the use of multielement linear transducer array enhances the collection efficiency, especially for three-dimensional PA imaging. Finally, it has the ability to reconstruct three-dimensional PA image of biology tissues with high contrast.

#### ACKNOWLEDGMENTS

This research is supported by the National Basic Research Program of China (2010CB732602; 2011CB910402), the Program for Changjiang Scholars and Innovative Research Team in University (IRT0829), and the National Natural Science Foundation of China (30870676).

<sup>1</sup>J. M. Yang, K. Maslov, H. C. Yang, Q. F. Zhou, and L. V. Wang, *Proc. SPIE* **7177**, 1 (2009).

<sup>2</sup>Y. G. Zeng, D. Xing, Y. Wang, B. Z. Yin, and Q. Chen, *Opt. Lett.* **2**, 1760 (2004).

<sup>3</sup>M. Yamazaki, S. Sato, H. Ashida, D. Saito, Y. Okada, and M. Obara, *J. Biomed. Opt.* **10**, 064011 (2005).

<sup>4</sup>Z. Yuan, Q. Z. Zhang, and H. B. Jiang, *Opt. Express* **14**, 6749 (2006).

<sup>5</sup>J. A. Viator, G. Paltauf, S. L. Jacques, and S. A. Prahl, *Proc. SPIE* **4256**, 16 (2001).

- <sup>6</sup>J. M. Yang, K. Maslov, H. C. Yang, Q. F. Zhou, K. K. Shung, and L. V. Wang, *Opt. Lett.* **34**, 1591 (2009).
- <sup>7</sup>S. Sethuraman, J. H. Amirian, S. H. Litovsky, R. W. Smalling, and S. Y. Emelianov, *Opt. Express* **15**, 16657 (2007).
- <sup>8</sup>J. L. Su, B. Wang, and S. Y. Emelianov, *Opt. Express* **17**, 19894 (2009).
- <sup>9</sup>Y. Yuan, S. H. Yang, and D. Xing, *Opt. Lett.* **35**, 2266 (2010).
- <sup>10</sup>D. W. Yang, D. Xing, S. H. Yang, and L. Z. Xiang, *Opt. Express* **15**, 15566 (2007).
- <sup>11</sup>H. Guo and S. H. Yang, *Rev. Sci. Instrum.* **80**, 014903 (2009).
- <sup>12</sup>A. A. Oraevsky, V. G. Andreev, A. A. Karabutov, and R. O. Esenaliev, *Proc. SPIE* **3601**, 256 (1999).
- <sup>13</sup>M. H. Xu and L. V. Wang, *IEEE Trans. Med. Imaging* **21**, 814 (2002).
- <sup>14</sup>D. W. Yang, D. Xing, H. M. Gu, Y. Tan, and L. M. Zeng, *Appl. Phys. Lett.* **87**, 194101 (2005).
- <sup>15</sup>Z. F. Ge, K. T. Schomacker, and N. S. Nishioka, *Appl. Spectrosc.* **52**, 833 (1998).
- <sup>16</sup>H. L. Ao, D. Xing, H. J. Wei, H. M. Gu, G. Y. Wu, and J. J. Lu, *Phys. Med. Biol.* **53**, 2197 (2008).